The Journal of CPRI,
Vol. 10, No. 4, December 2014 pp. 703-714

# Effect of static var compensator on the performance of digital distance relay protection of transmission line

Mohan P Thakre* and Vijay S Kale**

*This paper presents modelling of distance relay with static Var compensator (SVC) and investigates its impact on the apparent impedance seen by the transmission line distance relay. The functional structure for SVC built with a Thyristor Controlled Reactor (TCR) and its model are described. The model is based on representation of the controller as variable susceptance (BSVC) that changes with the firing angle of the TCR. SVC has a remarkable effect on the apparent impedance seen by the distance relay. The impact of SVC is more pronounced on the apparent impedance seen by the phase to ground fault. The mal-operation of the distance protection for the transmission line with SVC at various locations is studied. It is also shown that the primary winding connection of the interfacing transformer of the SVC has extraordinary effect on the apparent impedance seen by the relay. The simulation results show that the under-reaching and over-reaching is more severe with SVC at mid-point of the transmission line. The impact of SVC on the relay tripping boundaries is also clearly demonstrated.*

***Keywords:*** *Distance relay, transmission line protection, trip boundary, SVC, PSCAD/EMTDC software*

## 1.0 INTRODUCTION

The protection of the transmission line is an important aspect when we consider the stability of the power system as it is used to transfer bulk power from one area to other. The distance protection of the transmission line gives reliable and the fast decision making capability to detect fault in the zone of protection and provides the information about trip or no trip [1]. Distance Relaying belongs to the principle of ratio comparison. The ratio is between voltage and current, which in turn produces impedance. The impedance is proportional to the distance in transmission lines, hence the distance relaying designation for the principle. This principle is primarily used or protection of high voltage transmission lines.

Static Var Compensator (SVC) is one of the earliest Flexible AC Transmission System (FACTS) devices. It generates or absorbs reactive power at its point of connection, usually in the middle of a high voltage transmission line. Before the evolution of SVC in the 1960s, synchronous compensators performed such compensation [2]. Among the FACTS controllers, Static Var Compensator (SVC) provides fast acting dynamic reactive compensation for voltage support during contingency events, which would otherwise depress the voltage for a significant length of time. SVC also dampens power swings and reduces system losses by optimized reactive power control.

SVC regulates the voltage at its terminals by controlling the amount of reactive power injected

*Electrical Department, Visvesvaraya National Institute of Technology, Nagpur - 440010, India. E-mail : thakre_mohan@yahoo.com
**Electrical Department, Visvesvaraya National Institute of Technology, Nagpur - 440010 (MS), India. E-mail : tovijay_kale@yahoo.com

into or absorbed from the power system. When the system voltage is low, SVC generates reactive power (capacitive mode) and when the voltage is high, it absorb reactive power (inductive mode) [3]. However, the presence of SVC in a transmission line creates certain problems for the protective relays and fault locators because of the rapid changes introduced by the associated control actions. Apparent impedance seen by the distance relay is affected due to the variation of the voltage at the point of SVC connection. Distance relay characteristics are greatly subjected to mal-operation in the form of under-reaching and over reaching the fault point[4]. Generally, the impact of compensators on the transmission line protection is divided into series compensation, shunt compensation and series/shunt compensation. The impact of series compensation on the performance of conventional distance relay is presented in [5, 6]. The impact of shunt compensation on conventional distance protection is studied in [8-11]; on the other hand the impacts of series/shunt compensation devices are reported in [12, 13]. The main focus of sidhu et al.[10]is on the impact of STATCOM on the performance of distance relay.

In this work, the impact of SVC is investigated analytically by applying accurate modelling concepts which is missing in most of the literature in this regard, and then the analytical results are verified by detailed simulations. SVC control scheme is simulated by detailed transient models. Static models for SVC, as used in some published papers, does not accurately present the behaviour of SVC during a fault; hence the performance of the distance relay is not clearly evaluated in this case.

The paper is organized as follows. First a brief description of the system model and SVC control scheme is given in section 2. Section 3 provides an analytical procedure for different installation location of SVC using symmetrical analysis method. Effect of SVC on distance relay tripping characteristic and simulation results are provided in section 4 and 5 respectively. Finally, remedial action and the conclusion are given in section 6.

## 2.0 SYSTEM MODEL

The effect of the dynamics of the SVC and their associates controllers on the performance of distance relays are studied using the PSCAD/ EMTDC software. The study system and the modelling of the SVC control scheme are described in this section.

### 2.1 Study System

A power system model with the facility to vary the system strength, fault and SVC location, type of fault, load flow and direction of load is used so that all possible flow can be simulated and studied.

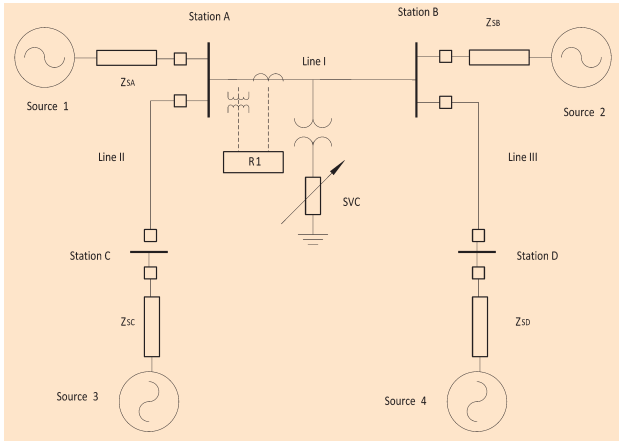


FIG. 1 SINGLE LINE DIAGRAM OF SAMPLE SYSTEM

Figure 1 shows the single line diagram of the system model considered for the analysis. The distance relay is located at station A, on Line I. The SVC installed is at the midpoint of the transmission Line I. The system data are shown in the Appendix.

### 2.2 SVC Controller Model

For the dynamic simulation study, 12 pulse SVC is considered. The power rating of FACTS controller is selected such that it can regulate the mid-point voltage and provide sufficient compensation for all conditions of loading and system strength. A slope of 3% is employed in their characteristic. The FACTS controller is connected to the transmission system via an

interfacing transformer as shown in Figure 1. To accurately model the FACTS controllers used in transmission system, a three phase balanced firing scheme is adopted. This implies that all the three phases are fixed at the same angle but 120 degree apart. Necessary filters have been provided in the FACTS controllers to limit the effects of system resonance and the harmonics [2, 3].

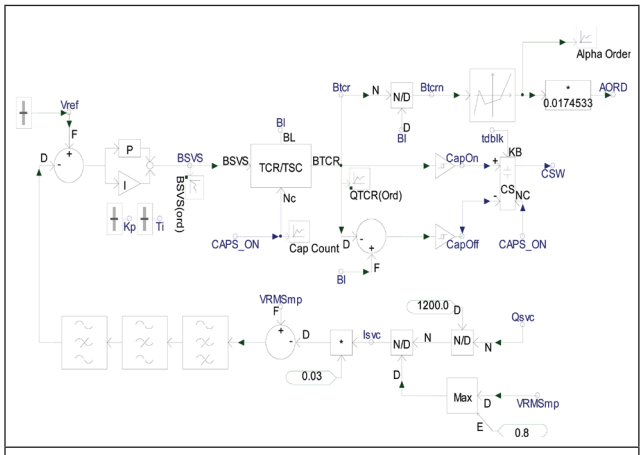


FIG. 2 SVC CONTROL SCHEME

The SVC comprises a thyristor switched capacitor (TSC) and thyristor controlled reactor (TCR) connected in parallel to the compensation point of the system. With proper co-ordination of the capacitor switching and reactor control, the reactive output can be varied continuously between the capacitive and inductiveratings.

SVC control scheme is presented in Figure 2. The technique by which the angle order is generated based on the changes in parameters of the main circuit. Utilizing this angle, the order required firing signals for SVC converter is generated. Measured reactive power and root mean square (RMS) voltage (in per unit) is given as the input. The measured reactive power is divided with the rated reactive power of the circuit. This output is divided with the measured RMS voltage (in per unit). After allowing a drop of about 3% the output of this block is summed up again with the measured RMS voltage. This summed output is passed through filters. The reference voltage (in p.u.), is summed with the output signal of the filters. This is given as input to the PI controller. The TCR/TSC unit in Figure 2 uses $B_{SVC}$ to determines the logic whether a TSC is to be switched in or out. Susceptance of TCR ($B_{TCR}$) is calculated from the SVC susceptance ($B_{SVC}$) and if $B_{TCR} \leq 0$, then a TSC is switched in. If $B_{TCR} \geq B_L$, then a TSC is switched out.

Generally, there are two operational modes of SVC

1. Var regulation mode: SVC reactive power is fixed in this case and SVC susceptance is kept constant. The presence of voltage regulator is not necessary in the control system in this mode, so $B_{SVC}$ is applied directly by external controller to the SVC[3].
2. Voltage regulation mode: In this mode $V_{Ref}$ value is specified by external controller. SVC holds output voltage in $V_{Ref}$ by absorbing or generating reactive power and it is performed by a PI regulator.

## 3.0 ANALYSIS OF SVC IMPACT ON THE MEASURED IMPEDANCE BY DISTANCE RELAY

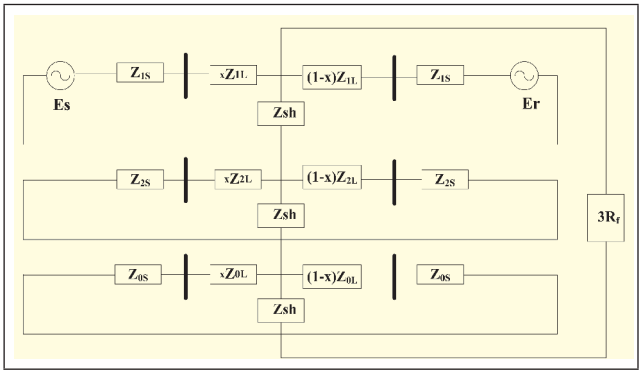


FIG. 3 EQUIVALENT CIRCUIT OF PHASE A TO GROUND FAULT WHEN SVC IS INSTALLED.

$Z_{1s}$, $Z_{2s}$, $Z_{0s}$ positive, negative and zero sequence impedance of sending end source respectively.

$Z_{1r}$, $Z_{2r}$, $Z_{0r}$ positive, negative and zero sequence impedance of receiving end source respectively.

$Z_{1L}$, $Z_{2L}$, $Z_{0L}$ positive, negative and zero sequence impedance of transmission line respectively.

$E_S$, $E_r$ sending and receiving end source voltage of $E_{SA}$ and $E_{SB}$ respectively

$Z_{sa}$ apparent impedance seen by distance relay for fault on Phase-A

$R_f$ fault resistance in ohm

$Z_{sh}$ SVC Shunt impedance

δ load angle

x per unit distance

Figure 3 shows that the equivalent circuit for phase A to ground fault, by using the symmetrical fault analysis method. The following equations are obtained when SVC is not installed in the system as:

$$Z_{s1} = Z_{1S} + xZ_{1L} \quad \text{....(1)}$$

$$Z_{R1} = Z_{1r} + (1-x)Z_{1L} \quad \text{....(2)}$$

$$Z_{s0} = Z_{0S} + xZ_{0L} \quad \text{....(3)}$$

$$Z_{R0} = Z_{0r} + (1-x)Z_{0L} \quad \text{....(4)}$$

$$Z_{\Sigma} = 2\frac{Z_{S1}Z_{R1}}{Z_{S1} + Z_{R1}} + \frac{Z_{S0}Z_{R0}}{Z_{S0} + Z_{R0}} \quad \text{....(5)}$$

$$C_{S1} = \frac{Z_{R1}}{Z_{S1} + Z_{R1}} \quad \text{....(6)}$$

$$C_{S0} = \frac{Z_{R0}}{Z_{S0} + Z_{R0}} \quad \text{....(7)}$$

$$K_{mo} = \frac{Z_{0L} - Z_{1L}}{3Z_{1L}} \quad \text{....(8)}$$

$$K_d = \frac{1 - he^{-j\delta}}{Z_{S1}he^{-j\delta} + Z_{R1}} \quad \text{....(9)}$$

$$C_{load} = \frac{Z_{\Sigma} + 3R_f}{k_d} \quad \text{....(10)}$$

$$Z_{Sa} = xZ_{1L} + \frac{3R_f}{[C_{load} + 2C_{S1} + C_{s0}(1 + 3K_{mo})]} \quad \text{....(11)}$$

From equation (11) it is seen that, the measured impedance by the distance relay between point S and fault point, is equal to the positive sequence impedance of transmission line in the absence of the fault resistance.

When SVC is connected in the transmission line the above equation will change. Impedance Zsa determined by the installation point of the SVC in the system. Figure 3 shows the equivalent circuit diagram for SVC location on the transmission line. Here, we have considered three different locations for the investigation of the ideal characteristics impedance seen by the distance relay.

### 3.1 SVC Installed at Near End

When SVC is installed at near end in the system, then Equation (1), (3) and (9) are changed as:

$$Z_{S1F} = Z_{1s} + xZ_{1L} \quad \text{....(12)}$$

$$Z_{sl1} = Z_{1s} \quad \text{....(13)}$$

$$Z_{S1} = xZ_{1L} + \frac{Z_{S1l}Z_{Sh}}{Z_{S1l} + Z_{Sh}} \quad \text{....(14)}$$

$$Z_{R1F} = Z_{1r} + (1-x)Z_{1L} \quad \text{....(15)}$$

$$Z_{S1lF} = xZ_{1L} \quad \text{....(16)}$$

$$Z_{S0} = xZ_{0L} + \frac{Z_{S0l}Z_{Sh}}{Z_{S0l} + Z_{Sh}} \quad \text{....(17)}$$

$$K_d = \frac{Z_{sh}\left[1 - he^{-j\delta}\right] - Z_{s1l}he^{-j\delta}}{Z_{sh}[Z_{s1F}he^{-j\delta} + Z_{R1F}] + Z_{s1F}Z_{s1l}he^{-j\delta}} \quad \text{....(18)}$$

From equation (18), it is reveal that when fault resistance is zero the effect of the SVC is not observed in the impedance measured by the distance relay.

The impedance measured is equal to the transmission line impedance. It is due to the fact that the SVC is installed at the near end of the line and when there is fault in the zone-1 of the distance relay, the SVC is not present in the fault loop.

### 3.2 SVC Installed at Mid-Point

Now, when SVC is installed at the mid-point of the transmission line, we have two cases, first when fault occurs between the relaying point and the SVC, second when fault occurs after the SVC or mid-point. In the first case, theSVC is not present in the fault loop and therefore the effect of SVC is not included in the impedance measured by distance relay. In the second case, the SVC is present in the fault loop and it affects the impedance measured by the distance relay. Now the equations for both the cases and the ideal impedance characteristic are different. For the first case equations (2), (4) and (9) are modified by introducing new equations as-

$$Z_{S1F} = Z_{1s} + xZ_{1L} \quad \text{....(19)}$$

$$Z_{R1F} = Z_{1r} + (1-x)Z_{1L} \quad \text{....(20)}$$

$$Z_{R1l} = Z_{1r} + 0.5Z_{1L} \quad \text{....(21)}$$

$$Z_{R1} = (0.5-x)Z_{1L} + \frac{Z_{R1l}Z_{Sh}}{Z_{R1l} + Z_{Sh}} \quad \text{....(22)}$$

$$Z_{S1lF} = (0.5-x)Z_{1L} \quad \text{....(23)}$$

$$Z_{R0} = (0.5-x)Z_{1L} + \frac{Z_{Sh}(Z_{0r} + 0.5Z_{0L})}{Z_{Sh} + Z_{0r} + 0.5Z_{0L}} \quad \text{....(24)}$$

$$K_d = \frac{Z_{sh}\left[1 - he^{-j\delta}\right] - Z_{R1l}}{Z_{sh}[Z_{s1F}he^{-j\delta} + Z_{R1F}] + Z_{s1F}Z_{R1l}} \quad \text{....(25)}$$

Similarly, for second case, when fault occurs between the mid-point and the far end of transmission line, the equations (1), (3), (9) and (11) are modified by introducing new equations as-

$$Z_{S1F} = Z_{1s} + xZ_{1L} \quad \text{....(26)}$$

$$Z_{S1l} = Z_{1s} + 0.5Z_{1L} \quad \text{....(27)}$$

$$Z_{S1} = (x-0.5)Z_{1L} + \frac{Z_{S1l}Z_{Sh}}{Z_{S1l} + Z_{Sh}} \quad \text{....(28)}$$

$$Z_{R1F} = Z_{1r} + (1-x)Z_{1L} \quad \text{....(29)}$$

$$Z_{S1lF} = (x-0.5)Z_{1L} \quad \text{....(30)}$$

$$Z_{R1l} = Z_{1r} + 0.5Z_{1L} \quad \text{....(31)}$$

$$Z_{S0} = (x-0.5)Z_{1L} + \frac{Z_{Sh}(Z_{0s} + 0.5Z_{0L})}{Z_{Sh} + Z_{0s} + 0.5Z_{0L}} \quad \text{....(32)}$$

$$C_{1S} = \frac{Z_{sh}}{Z_{sh} + Z_{s1l}} \quad \text{....(33)}$$

$$C_{0s} = \frac{Z_{sh}}{Z_{Sh} + Z_{S1l} + 0.5Z_{0L}} \quad \text{....(34)}$$

$$K_d = \frac{Z_{sh}\left[1 - he^{-j\delta}\right] - Z_{R1l}}{Z_{sh}[Z_{s1F}he^{-j\delta} + Z_{R1F}] + Z_{s1lF}Z_{S1l}he^{-j\delta}} \quad \text{....(35)}$$

$$\mathrm{K'_d} = \frac{-\left[\mathrm{Z_{s1l}he^{-j\delta} + Z_{R1l}}\right]}{\mathrm{Z_{sh}[Z_{s1F}he^{-j\delta} + Z_{R1F}] + Z_{s1lF}Z_{S1l}he^{-j\delta}}} \quad \text{....(36)}$$

$$C_{loadΔ} = \left(Z_{\sum} + 3R_f\right)K'_d \quad \text{....(37)}$$

$$\mathrm{C_{1lF} = Z_{S1lF}[C_{loadΔ} + 2C_{S1}(1 - C_{1s}) + C_{s0}(1 + 3K_{mo})(1 - C_{os})]} \quad \text{....(38)}$$

$$\mathrm{Z_{sa} = xZ_{1L} + \frac{C_{1lF} + 3R_f}{[C_{loadΔ} + 2C_{S1}C_{1s} + C_{s0}C_{os}(1 + 3K_{mo})]}} \quad \text{....(39)}$$

From equation (39), it is observed that, even in the absence of the fault resistance the measured impedance by the distance relay is affected by the SVC parameter.

### 3.3 SVC Installed at Far End

In this case the SVC is connected at the far end of the transmission line and hence SVC is not present in the fault loop. The equations (2), (4) and (9) are modified by introducing new equations as;

$$Z_{S1F} = Z_{1s} + xZ_{1L} \quad \text{....(40)}$$

$$Z_{R1F} = Z_{1r} + (1-x)Z_{1L} \quad \text{....(41)}$$

$$Z_{Rl1} = Z_{1r} \quad \text{....(42)}$$

$$Z_{R1} = (1-x)Z_{1L} + \frac{Z_{R1l}Z_{Sh}}{Z_{R1l} + Z_{Sh}} \quad \text{....(43)}$$

$$Z_{S1lF} = (1-x))Z_{1L} \quad \text{....(44)}$$

$$Z_{S0} = (1-x)Z_{0L} + \frac{Z_{Sh}(Z_{0r})}{Z_{Sh} + Z_{0r}} \quad \text{....(45)}$$

$$K_d = \frac{Z_{sh}\left[1 - he^{-j\delta}\right] - Z_{R1l}}{Z_{sh}[Z_{s1F}he^{-j\delta} + Z_{R1F}] + Z_{s1lF}Z_{R1l}} \quad \text{....(46)}$$

## 4.0 EFFECTS OF SVC ON DISTANCE RELAY TRIPPING CHARACTERISTIC

The impact of the presence of SVC on a transmission line has been tested for a practical system. A 400 kV transmission line I with the length of 300 km has been used for this study. The distance relay is located at Station A, as shown in Figure 1. Calculated impedances of transmission line and the other parameters of the power system are shown in the Appendix.

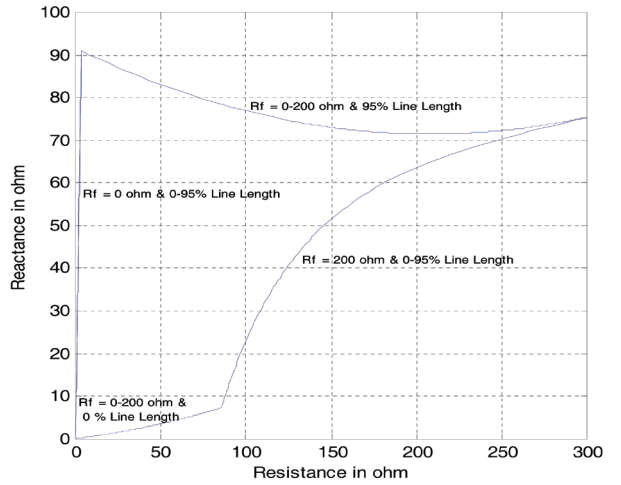


FIG. 4 TRIPPING CHARACTERISTIC, WITHOUT

In the absence of SVC, Figure 4 shows the tripping characteristic of the distance relay without SVC, for phase to ground faults. The measured impedance at the relaying point is plotted as the fault resistance changes from 0 to 200 ohms, while the fault location moves from the near end up to the far end of the transmission line [10].

Usually SVC controls their connecting point voltage according to their controlling strategy. Therefore, SVC parameters would vary as the power system loading is changed. But in this study the operational conditions of the power system are assumed to be constant. Here SVC compensation current is utilized to describe the operational condition. The lagging current is represented by the negative value while the leading current is shown by the positive value.

### 4.1 Device at Near End

Figure 5 shows the effect of SVC compensation variation on the measured impedance at the relaying point. Here, SVC compensation is 1.0, 0.5, 0.0, -0.5, and -1.0 per unit. It can be seen that in the case of an inactive SVC the measured impedance is not affected. It can be seen that as SVC current varies from the lagging to the leading mode, the measured reactance increases while the measured resistance decreases slightly. In the case of the low fault resistance, the measured impedance is approximately unchanged.

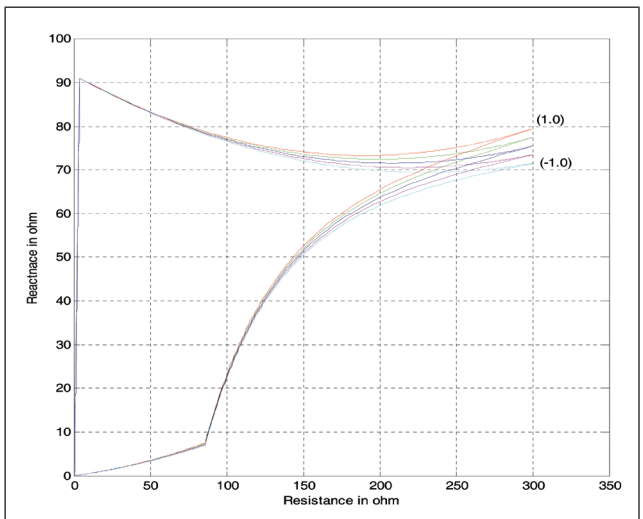


FIG. 5 TRIPPING CHARACTERISTIC, SVC AT

### 4.2 Device at Mid-Point

In this case, SVC is out of the fault loop for the faults on the near half of the line, while it is present in the fault loop for the faults on the far half. Figure 6 shows the effect of SVC compensation current variation on the tripping characteristic. Here, SVC compensation is 1.0, 0.5, 0.0, -0.5, and -1.0 per unit.

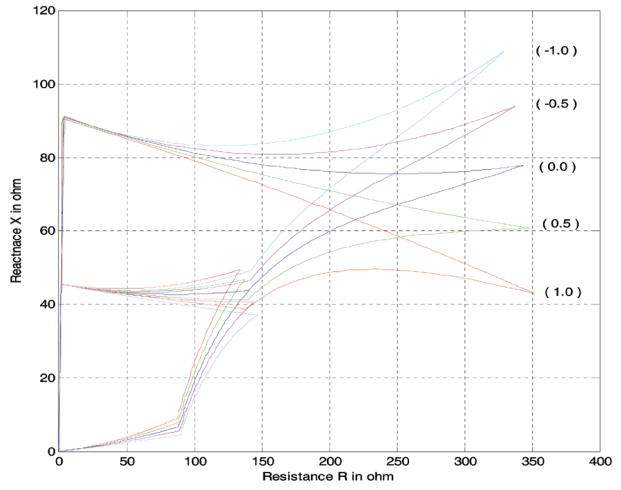


FIG. 6 TRIPPING CHARACTERISTIC, SVC AT

It can be seen that in the case of an inactive SVC the measured impedance is not affected. In the presence of SVC at the mid-point, the tripping characteristic is split into two adjoined parts. The lower part is for the faults on the near half of the line, while the upper part is corresponding to the faults on the far half. The lower boundary of the upper part and the upper boundary of the lower part are the same.

In the lower part, as SVC compensation current increase in the leading mode, the measured resistance increases slightly, while the measured reactance decreases more considerably. On the other hand and in the case of the lagging mode, as SVC compensation current increases, the measured resistance decreases slightly, while the measured reactance increases more considerably. In the case of low fault resistances, the measured impedance is approximately unchanged.

In the upper part, as SVC compensation current increase in the leading mode, the measured resistance increases slightly. In the case of the measured reactance, it decreases for the fault close to the mid-point, and for the faults close to the far end, it increases for low fault resistances while it decreases in the case of high fault resistances. On the other hand and in the lagging mode, as SVC compensation current increases the measured resistance decreases slightly, in the case of the measured reactance, it increases for the faults closed to the mid-point, and for the faults closed to the far end, it decrease for low fault resistances while it increases in the case of high fault resistances.

### 4.3 Device at Far End

Figure 7 shows the effect of SVC compensation variation on the measured impedance at the relaying point. Here, SVC compensation is 1.0, 0.5, 0.0, - 0.5, and -1.0 per unit. It can be seen that in the case of an inactive SVC the measured impedance is not affected.

It can be seen that as the operational mode varies from the lagging to the leading mode, the measured reactance decreases, while the measured resistance increases slightly. So from all these results obtained for tripping characteristic, it is found that the conventional MHO distance relay operation is not much affected by the SVC when it is not in the fault loop. But when SVC comes in the fault loop, the conventional

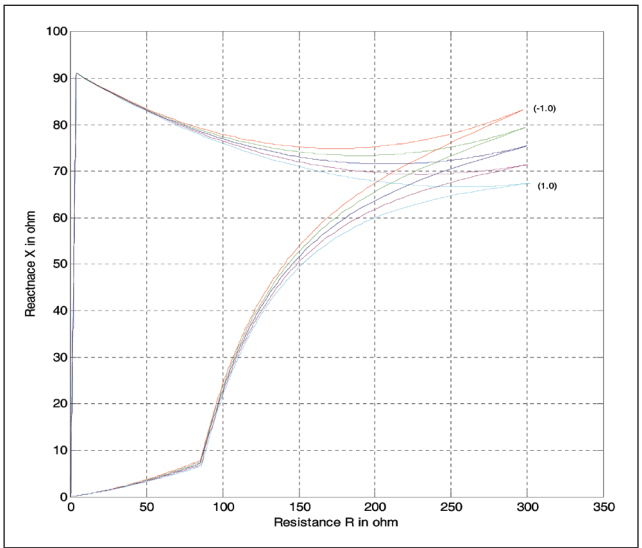


FIG. 7 TRIPPING CHARACTERISTIC, SVC AT FAR END

Mho distance relay mal-operates in the form of under-reaching and over-reaching in the fault point.

### 4.4 Distance Relay Modelling

The distance relay model is developed, where three phase voltages and currents are passed through anti-aliasing low-pass filters [14], then the phasors are extracted using Full Cycle Discrete Fourier Transform (FCDFT). Finally, after calculation the positive, negative and zero sequence components of the estimated phasors, the apparent impedances for the six measuring units (A-G, B-G, C-G, A-B, B-C, and C-A) are evaluated. The distance relay function which is emulated using PSCAD/EMTDC software is shown in Figure 8. This figure exhibits only A-G and A-B measuring unit as demonstrated.

The line to be protected 100 km from station A to station B, the relay setting with three mho zones with the following setting criteria:

Zone 1= 80% (80 km), with instantaneous time delay

Zone 2= 150% (150 km), with time delay in ms

Zone 3= 225% (225 km), with time delay in ms

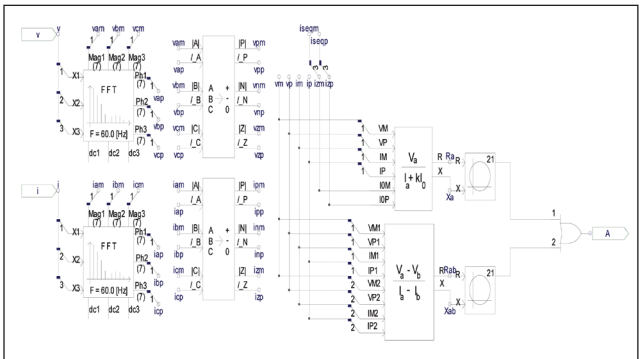

FIG. 8 RELAY MODEL (A-G & A-B MEASURING UNIT)

## 5.0 SIMULATION RESULTS

PSCAD/EMTDC an enrichment design tool software, used for modelling and simulating the power system. Figure 9 shows that the performance of SVC, when the circuit breaker open on load side at 0.2 sec, the SVC regulate the voltage at it terminals by the controlling the amount of reactive power absorbed from the power system. It means that when the voltage is high, it absorbed reactive power (inductive mode).

By controlling the firing angle α of the thyristors, the device is able to control the bus voltage magnitude. Changes in α result in changes on the current and hence, the amount of reactive power consumed by the inductor. When $\alpha=90^0$, the inductor is fully activated but is deactivate when $\alpha=180^0$. Actually, the basic control strategy is typically to keep the transmission bus voltage within certain narrow limit defined by a controller drop and the firing angle α limits ($90^0 < \alpha > 180^0$).

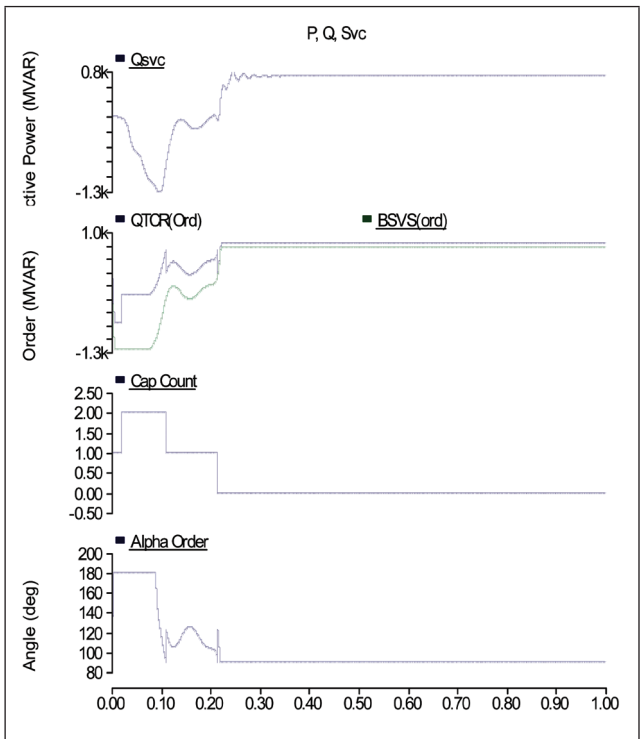


FIG. 9 PERFORMANCE OF SVC

### 5.1 Double Line Fault

For an A-B fault occurred at 0.2 sec at 140 km i.e. in Zone 2 from the relay, the apparent impedance calculated by A-B measuring unit is presented in Figure 10, which shows that with and without SVC trajectory, the presence of SVC in the fault loop does not have an appreciable impact.

Real and imaginary parts of phase to phase impedance are shown in Figure 11. As can be deduced from this figure the effect of phase to phase fault on the apparent impedance is negligible.

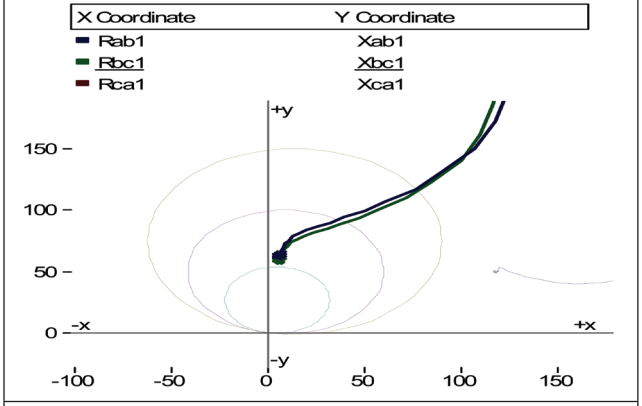


FIG. 10 APPARENT IMPEDANCE TRAJECTORY OF A-B MEASURING UNIT(LEGEND: GREEN=WITHOUT SVC, BLUE=WITH SVC)

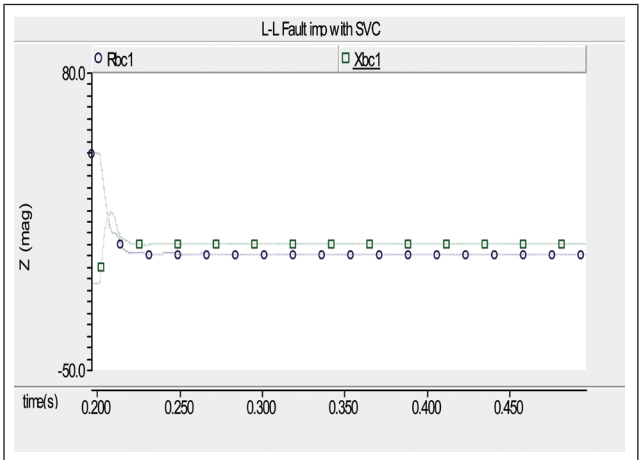


FIG. 11 REAL AND IMAGINARY PARTS OF APPARENT IMPEDANCE FOR AN A-B FAULT

## 5.2 Single Line to Ground Fault

For an A-G fault occurred in Zone 3 from the relay. Figure 12 shows the apparent impedance calculated by A-G measuring unit, which shows that with and without SVC trajectory, the presence of SVC in the fault loop and its injected capacitive current, force the relay to under-reach.

This is due to the zero-sequence component of the injected current increases; this current has a direct impact on the apparent impedance. Real and imaginary parts are also extracted for this A-G fault and are shown in Figure 13. Comparing the results of Figures. 12 and 13 indicates the consistency between them.

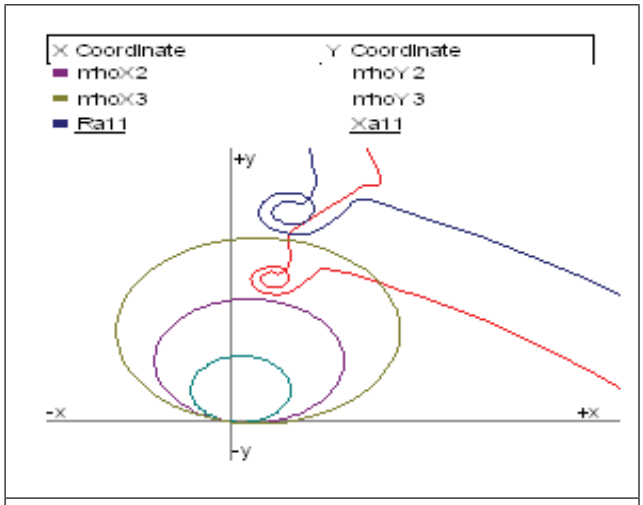


FIG. 12 APPARENT IMPEDANCE TRAJECTORY OF A-G MEASURING UNIT (LEGEND: RED = WITHOUT SVC, BLUE = WITH SVC)

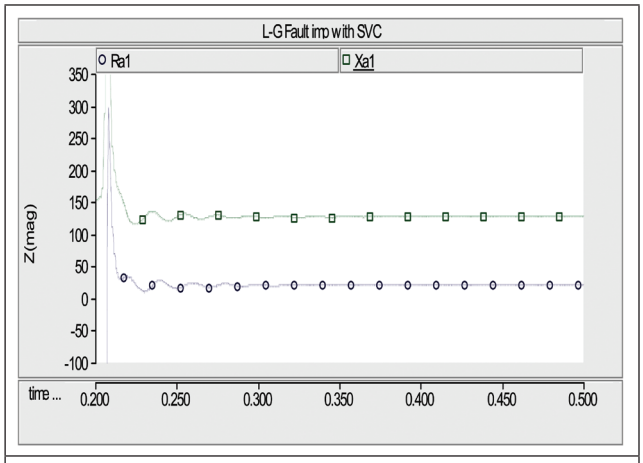


FIG. 13 REAL AND IMAGINARY PARTS OF APPARENT IMPEDANCE FOR AN A-G FAULT

## 5.3 Load Angle and System Short Circuit Level (SCL)

Figure 14 shows apparent impedance calculated by A-G measuring unit, for an A-G fault occurred at 0.2 sec at 150km from the relay and different load angle with presence of SVC. As can be seen from this figure, SVC increases the R/X value by increasing the load angle from 200 to 600. So by observing the trajectory it is concluded that Mho distance relay is over-reaching the fault point. As the load angle increase the deviation are more severe and distance relay mal-operates. For different system SCLs with presence of SVC and the same A-G fault occurred at zone 3. As can be seen from Figure 15, the impact of SVC

on the apparent impedance is significant for weak system and this impact is severe on the apparent reactance. This is due to the fact that fault current are higher for strong systems in comparison to the weak systems. Therefore in systems with small SCL, the SVC injected capacitivecurrents are appreciable in comparison to the fault currents.

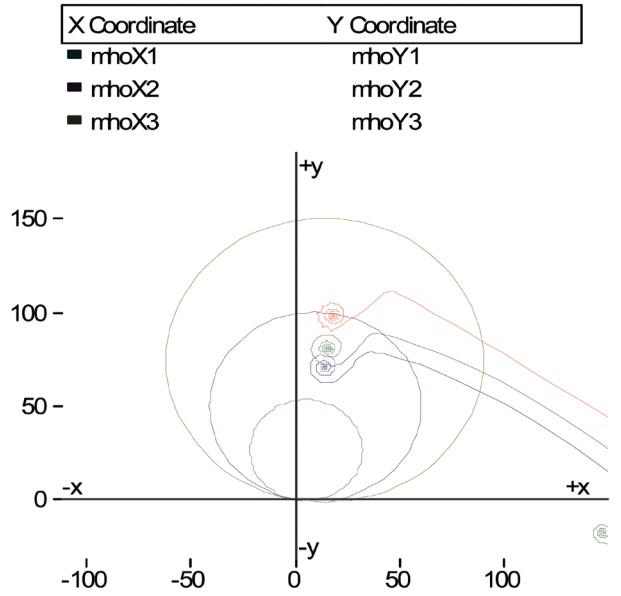


FIG. 14 APPARENT IMPEDANCE TRAJECTORY OF A-G MEASURING UNIT FOR DIFFERENT LOAD ANGLE VARIATION (LEGEND: RED =200, GREEN=400, BLUE=600)

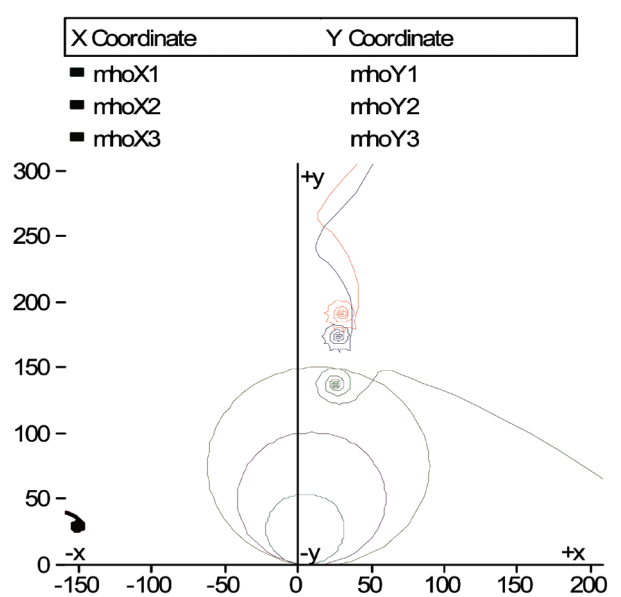


FIG. 15 APPARENT IMPEDANCE TRAJECTORY OF A-G MEASURING UNIT FOR DIFFERENT SCLS VARIATION (LEGEND: GREEN=WITHOUT SVC, BLUE=SCL 2000 MVA WITH SVC, GREEN= SCL 8000MVA WITH SVC)

## 5.4 Setting Effect of SVC

Figure 16 shows the apparent impedance trajectory for variation of reference voltage by SVC. For an A-G fault occurred at 0.2 sec at Zone 2 from the relay, when the SVC voltage setting (Vref) are 0.85 and 1.05 p.u., respectively. As can be seen from Figure 16, when SVC is connected at the mid-point of the transmission line and working in capacitive or inductive mode, the measured impedance seen by the relay is out of the zone 2 of line. This causes the mal-operation of the distance relay in the form of under-reaching and over-reaching respectively.

As fault resistance increases the deviation are more severe and distance relay mal-operate in both the cases to detect accurate fault locationin the form of under-reaching and over-reaching.

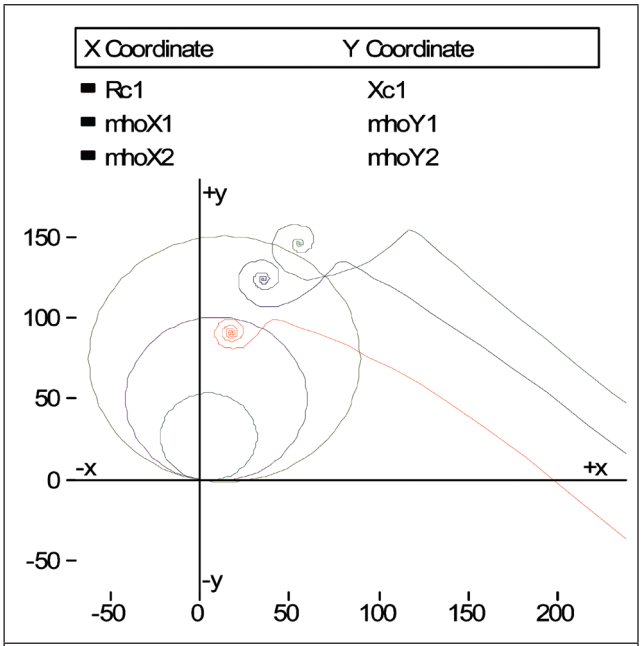


FIG. 16 APPARENT IMPEDANCE TRAJECTORY OF A-G MEASURING UNIT FOR DIFFERENT REFERENCE VOLTAGES (LEGEND: RED=WITHOUT SVC, BLUE= WITH SVC VREF = 0.85P.U, GREEN = WITH SVC VREF = 1.05P.U))

## 5.5 Coupling Transformer Connection Primary Side

In order to demonstrate the effect of zero-sequence component on the apparent impedance trajectory seen by the relay, the connection type of the SVC coupling transformer could be selected in such

a way as to rectify the impact of zero-sequence component. Suppose the transformer primary connection could be changed from Yg to Y. The same results are simulated and shown in Figure 17 for the same A–G fault for this new connection; it can be clearly deduced that the SVC impact is diminished significantly.

The impact of SVC coupling transformer of primary connection (Yg) on the calculated impedance, due to the zero-sequence component of the injected current by the SVC as shown in Figure 17. If the SVC is bypassed during the time that the zero-sequence component of the SVC current is increased, then SVC would have no effect on the apparent impedance. In order to recognize the zero-sequence component of the SVC current, the earth-fault relay could be used in the SVC current path [15]. By using an earth-fault relay in the SVC current path to detect and

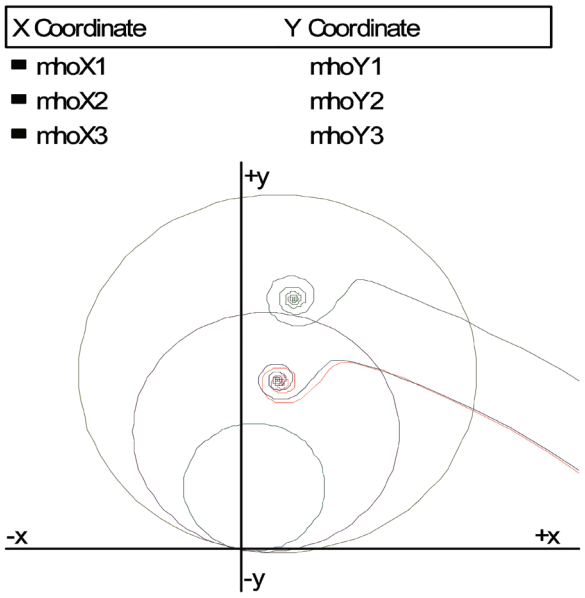


FIG. 17 APPARENT IMPEDANCE TRAJECTORY OF A-G MEASURING UNIT FOR DIFFERENT PRIMARY CONNECTION OF COUPLING TRANSFORMER (LEGEND: RED=WITHOUT SVC, BLUE= WITH SVC & Y/Δ TRANSFORMER, GREEN= WITH SVC & YG/ΔTRANSFORMER)

bypass the SVC, so there is no effect on the calculated impedance of the distance relay.

## 6.0 CONCLUSION

In this paper SVC impact on distance relay have been investigated through desirable simulation. It becomes clear that the impact of SVC is more pronounced on the apparent impedance seen by the phase to ground fault measuring units than the SVC coupling transformer primary connection. If the winding connection of the SVC coupling transformer is changed from Yg/Δ to Y/Δ, then the zero sequence current in the primary connection of the coupling transformer would be zero, so the impact of SVC on the apparent impedance for an A-G Fault with low Rf values is mitigated.

From the result described in this paper, it can be observed that the location of SVC as well as configuration and fault location affect the accuracy of distance relay. The trip boundaries of the phase to ground fault measuring units of the relay are influence by the presence of the SVC. Therefore, to provide a suitable trip boundary need to be adaptively magnitude with the zero sequence current in the primary connection of the coupling transformer of the SVC.

## APPENDIX

System Data of Figure 1

- Equivalent Sources ( 1, 2, 3 & 4 )

  Power rating = 100 MVA

  System voltage = 400kV

  System frequency = 60 Hz

  Positive seq. Impedance = $25.9\angle 80^{0}$^0 Ω/km

  Zero seq. impedance = $25.9\angle 80^{0}$^0 Ω/km
- Transmission line (I,II,III)

  Line length = 300 km

  Positive seq. Impedance = $0.788969\angle 81.63^{0}$ ^0 Ω/km

  Zero seq. impedance = $0.2939\angle 68.20^{0}$^0Ω/km
- FACTS Device (SVC)

  Interfacing transformer = 3 winding (Y/y/d)

  Transformer ratio = 400/12.65/12.65 kV

  Transformer rating = 200 MVA

  Transformer impedance = 0.1 p.u.

  SVC capacitive rating = 167 MVA

  SVC inductive rating = 100 MVA

## REFERENCE


[1] Soman S.A.,"Power System Protection." Nptel<http://www.ddenptel.thapar.edu/courses/Webcourse-contents>.

[2] Hingorani and N G, Gyugyi L, "Understanding FACTS: Concepts and Technology of Fexible AC Transmission systems." New York: Wiley; 1999

[3] Padiyar K R, "FACTS Controllers in Power Transmission and Distribution." New Age International Publishers, 2007

[4] Waikar DL, Elangovan S, Liew A C, "Fault Impedance Estimation Algorithm for Digital Distance Relaying." IEEE Trans. Power Deliv., pp.1375–83, 1994

[5] Khederzadeh M, Sidhu T S., "Impact of TCSC on the Protection of Transmission Lines", IEEE Trans. Power Deliv., pp. 80–87, 2006

[6] Dash PK, Pradhan AK, Panda G, Liew AC., "Digital Protection of Power Transmission Lines in the Presence of Series Connected FACTS Devise," In: Proc IEEE power engineering soc winter meeting, vol. 3, pp.1967-1972, Jan 2000

[7] Albasri F A , Sidhu T S , Varma R K "Impact of Shunt-FACTS on Distance Protection of Transmission Lines." In: Proc. 2006 power systems conference: advanced metering, protection, control, communication, and distributed resources, PS 06; 2006, pp. 249–256, 2006

[8] El-Arroudi K, Joos G, Mc Gillis D T, "Operation of Impedance Protection Relays with the STATCOM." IEEE Tran. Power Deliv.; 17(2), pp.381–387, 2002

[9] Albasri F A, Sidhu T S, Varma R K., "Performance Comparison of Distance Protection Schemes for Shunt-FACTS Compensated Transmission Lines." IEEE Trans Power Deliv pp. 2116–2125, 2007

[10] Sidhu T S , Varma R K, Gangadharan PK, Albasri FA, Ortiz GR., "Performance of Distance Relays on Shunt-FACTS Compensated Transmission Lines." IEEE Trans Power Delivery, pp.1837–1845, 2005

[11] Khederzadeh M, Ghorbani A., "STATCOM Modelling Impacts on Performance Evaluation of Distance Protection of Transmission Lines." Euro Trans Elect. Power, pp.2063-2079, 2011

[12] Zhou X, Wang H, Aggarwal R K, Beaumont P., "Performance Evaluation of a Distance Relay as Applied to a Transmission System with UPFC." IEEE Trans Power Deliv 2006; 21(3): Pp. 1137–1147,2006

[13] Khederzadeh M , "The Impact of FACTS Device on Digital Multifunctional Protective Relays." In: Proc. IEEE power eng. soc. transmission and distribution conf. exhibit. Asia Pacific, vol. 3, Oct. 2002. pp. 2043–2048, Oct. 2002.

[14] Manitoba HVDC Research Centre, "PSCAD/EMTDC 4.2 Electromagnetic transients program including dc systems," 2003.

[15] Power system protection. Vol.2. Edited by The Electricity Training Association.